Open Access

Charge Carriers Compensation in a Ferromagnetic Mn-Implanted Si

A.F. Orlov[*,1], L.A. Balagurov[1], I.V. Kulemanov[1], Yu.N. Parkhomenko[1], A.V. Kartavykh[2], V.V. Saraikin[3], Yu.A. Agafonov[4] and V.I. Zinenko[4]

[1]State Institute for Rare Metals, Moscow, 119017, Russia

[2]Institute for Chemical Problems of Microelectronics, Moscow, 119017, Russia

[3]State Research Institute of Physical Problems, Zelenograd, Moscow, 103460, Russia

[4]Institute of Microelectronics Technology and High Purity Materials, Chernogolovka, Moscow Region, 142432, Russia

Abstract: Secondary ions mass-spectrometry and spreading resistance profiles in the layers of a ferromagnetic Si implanted with Mn has been studied. Czochralski Si wafers both n- and p-type, of high- and low-resistivity, as well as a float zone Si were implanted with impurity fluencies of (1 - 5) x 10^{16} cm^{-2}. The Mn impurity was found to compensate acceptors in a high-resistivity *p*-Si and donors in a low-resistivity *n*-Si. Only the small part of Mn ions in Si apparently incorporates into the Si crystal lattice, occupies the interstitial sites and the appropriate energy levels $(Mn_i)^{-/0}$ and $(Mn_i)^{+/++}$ equal to $E_c - 0.12$ eV for *n*-type Si and $E_v + 0.32$ eV for *p*-type Si, respectively, are activated after vacuum annealing.

PACS: 61.72.uf; 71.55.Cu; 72.20.Jv

Keywords: Ferromagnetic Si, implantation of Mn, spreading resistance, energy levels.

INTRODUCTION

Diluted ferromagnetic semiconductors keeping a ferromagnetic ordering at above room temperature are considered as the most promising material for creation semiconductor spin electronics devices. Especially, it concerns the ferromagnetic Si due to its technical compatibility in the present mature microelectronics technique. Room temperature ferromagnetism in Si doped with Mn have been firstly reported in [1, 2]. Authors [1] have made the crystalline $Mn_{0.05}Si_{0.95}$ films at Si (001) substrate by vacuum deposition followed by post-crystallization processing. The films were ferromagnetic ones with the Curie temperature over 400 K and the magnetization up to 1.3 emu/g. Above room temperature ferromagnetism of implanted with Mn commercial single-crystal Si wafers has been observed in [2, 3]. The structure, magnetic and magneto-optic properties of a ferromagnetic Si have been investigated in [3-9].

For application of such materials in devices of spin electronics it is very important to know the depth profiles of structural and physical properties in the ferromagnetic layer. The resistivity and carrier concentration profiles of starting commercially available *p*-type Si wafers with an initial resistivity of 600 Ω.cm, implanted with Mn and annealed, were measured in [10] by spreading resistance profiling (SRP). The resistivity of wafers was found to be enhanced by several times for Mn-doped material. The magnetic properties of this material have not been investigated. In this paper, we report the results of study the resistivity profiles in the above room temperature ferromagnetic Si *n*- and *p*-types both of high- and low-resistivity, implanted with impurities of Mn (Co). The magnetic and magneto-optic properties of these materials have been published earlier [8].

MATERIALS AND METODOLOGY

Commercially available Si wafers grown by the Czochralski method both *n*-type with the standard resistivity of 0.01 (doped with Sb) and 4.5 Ω.cm (doped with P) and *p*-type with the resistivity of 0.005 and 10 Ω.cm (both doped with B) as well as very high resistivity float zone *n*-type Si substrates were used as the starting materials. The materials were implanted with the impurities of Mn (or Co) at the ion energy of 195 keV and the fluencies in the range of (1, 2, and 5) x 10^{16} cm^{-2} at the temperature of 350 ^{0}C. After implantation, part of the samples were annealed in vacuum at 850 ^{0}C, 5 min. Measurements of the impurities concentration profiles were performed by using the Secondary ion mass spectrometer (SIMS) IMS-4F and SRP – measurements were carried out with ASR-100C.

RESULTS AND DISCUSSION

Fig. (**1**) depicts the Mn depth profiles in Si matrix for the samples after implantation with different fluencies and annealed and (insert) for the sample as-implanted at the fluency of 5 x 10^{16} cm^{-2} and for the same sample after following anneal. Before annealing, the profiles show a typical gaussian-like distribution with a projected range of 180 nm. An augmentation of the implantation fluency leads to increase of the Mn concentration value in maximum and to expansion of the profile. After annealing, as well as in [4], the Mn redistributes giving rise to “shoulders” on the right side of the main peak. This phenomenon has been described earlier as the segregation of implanted species as recrystallization fronts move through the material [11].

*Address correspondence to this author at the State Institute for Rare Metals, B.Tolmachevsky lane, 119017 Moscow, Russia;
E-mail: rmdp@girmet.ru

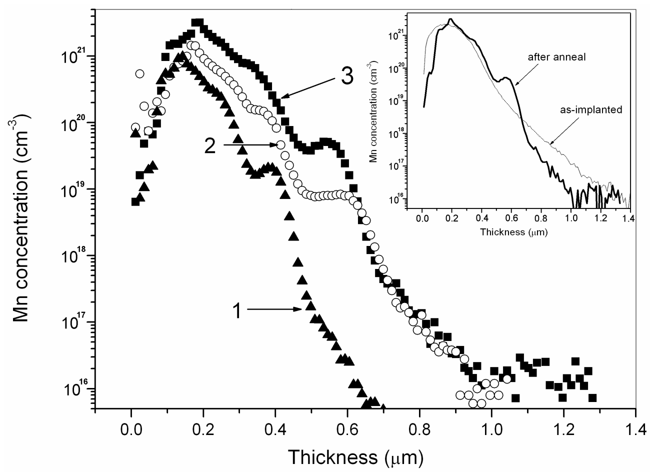

Fig. (1). SIMS-profiles of Mn, implanted in Si with different fluences of (1; 2 ; and 5) x 10^{16} cm^{-2} after vacuum annealing. 1- 1 x 10^{16}, 2- 2 x 10^{16}, 3- 5 x 10^{16} cm^{-2}. Insert: SIMS-profiles of Mn, implanted in Si with the fluence of 5 x 10^{16} cm^{-2}, before and after vacuum annealing at 850 $^{\circ}$C, 5 min.

Spreading resistance profiles were measured both in as-implanted and annealed samples. The curve in Fig. (**2**) presents the resistivity changing across the implanted layer of very high-resistivity (4.2 kΩ.cm) *n*-type float zone Si at the Mn fluency of 2 x 10^{16} cm^{-2} and annealed at 850 ^{0}C, 5 min. Up to the depth of 0.6 μm one can see the decrease of *n*-type Si resistivity down to 20 Ω.cm. Since the material is a float zone Si, the effect can not be caused by oxygen thermodonors and the reason of it may be donors of Mn impurity. Fig. (**3**) shows the resistivity profiles in the high-resistivity *p*- and *n*-type Si after implantation with Mn at the fluency of 2 x 10^{16} cm^{-2} and the following anneal. The hole compensation in *p*-type Si is observed up to the depth of 0.3 μm. The comparison with the appropriate curve at Fig. (**1**) shows that the compensation completely ceases approximately at the Mn concentration of 1 x 10^{17} cm^{-3}. Since the B concentration in the sample is equal to 1.5 x 10^{15} cm^{-3}, rather small part of Mn ions takes part into the hole compensation. Changing of the manganese for cobalt at implantation of such Si leads to the greater hole compensation (Fig. **4**). However, only the small compensation was found in the as-implanted Si (Fig. **4**), which indicates on activation of Mn impurity by the used short vacuum anneal. In the low-resistivity Si, as it is seen in Fig. (**5**), in the contrary to high-resistivity Si, the electron compensation was discovered after implantation with Mn and anneal. The compensation ceases at Mn concentration of 3 x 10^{20} cm^{-3} and the Sb concentration equal to 5 x 10^{18} cm^{-3}. Therefore, as well as in the case of *p*-type Si, only the small part of Mn ions displays an electroactivity. The comparison of Figs. (**3**, **5**) shows that Mn reveals the properties of an amphoteric impurity and compensates acceptors in a high-resistivity *p*-Si and donors in a low-resistivity *n*-Si.

The observed resistivity values in Mn-compensated parts of Si layers closely correspond to the values of energy levels equal to E_c – 0.12 eV for *n*-type Si and E_v + 0.32 eV for *p*-type Si. The amphoteric character of Mn-impurity in Si is well known. Ions of Mn in Si create donor levels $(Mn_i)^{0/+}$ and $(Mn_i)^{+/++}$ for interstitial sites in the crystal lattice and $(Mn_s)^{0/+}$ for substitutional sites. The energies of these levels are equal to 0.43 eV below the bottom of conductivity band for $(Mn_i)^{0/+}$ and two rest situated in the lower half of the forbidden band at 0.27-0.32 eV and 0.34 eV, correspondingly, above the floor of valence band [3, 12, 13]. The sole acceptor level $(Mn_i)^{-/0}$ for Mn in Si was found to be situated at 0.11 - 0.13 eV below the bottom of conductivity band [13, 14]. Thus, one can suppose that Mn ions in the materials under consideration occupy the interstitial sites and the energy levels $(Mn_i)^{-/0}$ and $(Mn_i)^{+/++}$ are activated in the low- and high-resistivity Si, respectively.

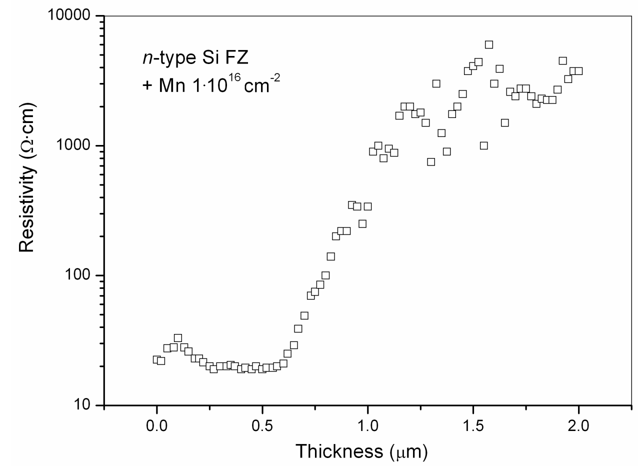

Fig. (2). Resistivity profile in the layer of the float zone Si, implanted with Mn at the fluency of 1 x 10^{16} cm^{-2} and annealed.

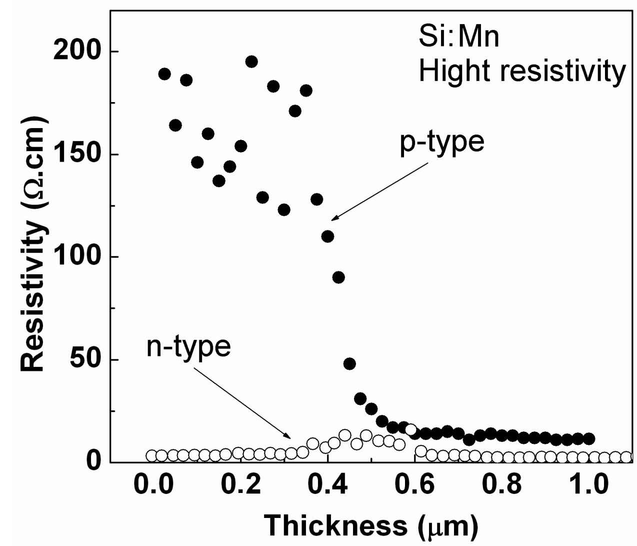

Fig. (3). Resistivity profiles in the layers of high-resistivity *n* - and *p* -type Si, implanted with Mn at the fluence of 2 x 10^{16} cm^{-2} and annealed.

As it can be seen in Figs. (**3**, **5**), the small increase of resistivity is observed in the implanted Si layers both *n*- and *p*-type conductivity at the depths in the range of 0.3-0.5 μm. The comparison with Fig. (**1**) indicates that the position of such augmentation at the abscissa axis at different fluencies of implanted Mn close correlates with the position of shoulders on the right part of Mn distribution curves. The reason of such resistivity augmentation can be the well known increase of crystal defects density (end-of-range defects) and the appropriate decrease of charge carriers mobility in the regions of crystallization fronts.

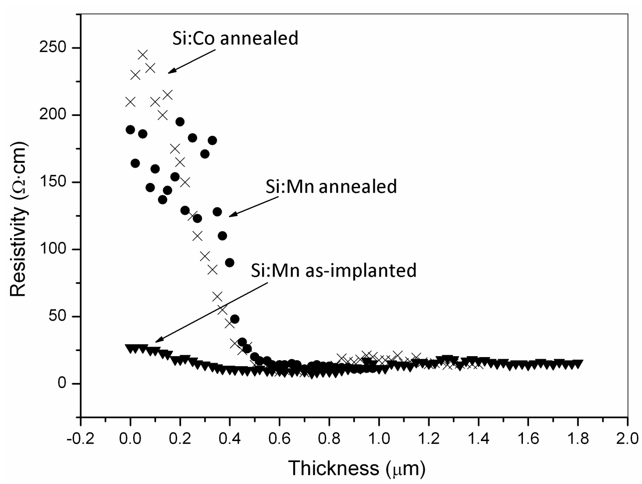

Fig. (4). Resistivity profiles in the layers of high-resistivity *p*-type Si, implanted with either Co 1 x 10^{16} cm^{-2} and annealed or Mn 2 x 10^{16} cm^{-2} (as-implanted or annealed).

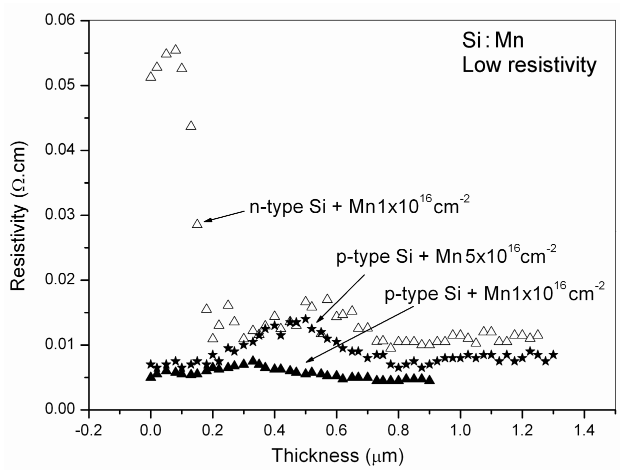

Fig. (5). Resistivity profiles in the layers of low-resistivity *n*- and *p*-type Si, implanted with Mn and annealed.

CONCLUSIONS

Spreading resistance profiles in the ferromagnetic layers of Mn-implanted Si wafers both n- and p-type of a various resistivity have been investigated. Mn-impurity in Si was found to reveal the amphoteric behaviour. The small part of implanted Mn ions after annealing apparently occupy the interstitial sites in Si crystal lattice and create the energy levels $(Mn_i)^{-/0}$ in the *n*-type Si and $(Mn_i)^{+/++}$ in *p*-type.

AKNOWLEDGEMENTS

The authors would like to thank Mrs. I.Yur'eva for preparation of the samples for measurements. The work was supported by the Russian Foundation for Basic Research, project #07-02-00327.

REFERENCES

[1] Zhang FM, Liu XC, Gao J, *et al.* Investigation on the magnetic and electrical properties of crystalline $Mn_{0.05}Si_{0.95}$ films. Appl Phys Lett 2004; 85: 786-8.

[2] Bolduc M, Awo-Affouda C, Stollenwerk A, *et al.* Above room temperature ferromagnetism in Mn-ion implanted Si. Phys Rev B 2005; 71: 033302-6.

[3] Yoon IT, Park CJ, Kang TW. Magnetic and optical properties of Mn-implanted Si material. J Magn Magn Mater 2007; 311: 693-6.

[4] Bolduc M, Awo-Affouda C, Stollenwerk A, *et al.* Magnetic and structural properties of Mn-implanted Si. Nucl Instrum Meth Phys Res B 2006; 242: 367-70.

[5] Bandaru PR, Park J, Lee JS, *et al.* Enhanced room temperature ferromagnetism in Co- and Mn-ion-implanted Si. Appl Phys Lett 2006; 89: 112502.

[6] Wolska A, Lawniczak-Jablonska K, Klepka M, *et al.* Local structure around Mn atoms in Si crystals implanted with Mn^+ studied using x-ray absorption spectroscopy techniques. Phys Rev B 2007; 75: 113201-4.

[7] Demidov ES, Danilov YuA, Podolsky VV, *et al.* Ferromagnetizm in the epitacsial layers of germanium and silicon, oversaturated with impurities of manganese and ferrum. JETP Lett 2006; 83: 664-7.

[8] Granovsky AB, Suhorukov YuP, Orlov AF, *et al.* Ferromagnetizm of silicon implanted with Mn: magnetization and Faraday magneto-optical effect. JETP Lett 2007; 85: 335-8.

[9] Shengqiang Z, Potzger K, Zhang G, *et al.* Structural and magnetic properties of Mn-implanted Si. Phys Rev B 2007; 75: 085203-15.

[10] Malik K, de Groot CH, Ashburn P, Wilshaw PR. Enhancement of resistivity of Czochralski silicon by deep level manganese doping. Appl Phys Lett 2006; 89: 112122-4.

[11] Bader R, Kalbitzer S. Carrier concentration profiles of ion-implanted Si. Appl Phys Lett 1970; 16: 13-5.

[12] Lemke H. Eigensehaften der dotierungsniveaus von mangan und vanadium in silizium. Phys State Solid 1981; A 64: 549-56.

[13] Czaputa R, Feihtinger H, Oswald J. Energy levels of interstitial manganese in silicon. Solid State Commun 1983; 47: 223-6.

[14] Fistul VI. Impurities in semiconductors: solubility, migration, and interactions. New York – London: CRC Press 2005.

Received: November 28, 2008 Revised: March 16, 2009 Accepted: March 17, 2009